

Supplemental Figures S1-14: Sensory processing in humans and mice fluctuates between external and internal modes

Authors:

Veith Weilnhammer^{1,2,3}, Heiner Stuke^{1,2}, Kai Standvoss¹, Philipp Sterzer⁴

Affiliations:

¹ Department of Psychiatry, Charité-Universitätsmedizin Berlin, corporate member of Freie Universität Berlin and Humboldt-Universität zu Berlin, 10117 Berlin, Germany

² Berlin Institute of Health, Charité-Universitätsmedizin Berlin and Max Delbrück Center, 10178 Berlin, Germany

³ Helen Wills Neuroscience Institute, University of California Berkeley, USA

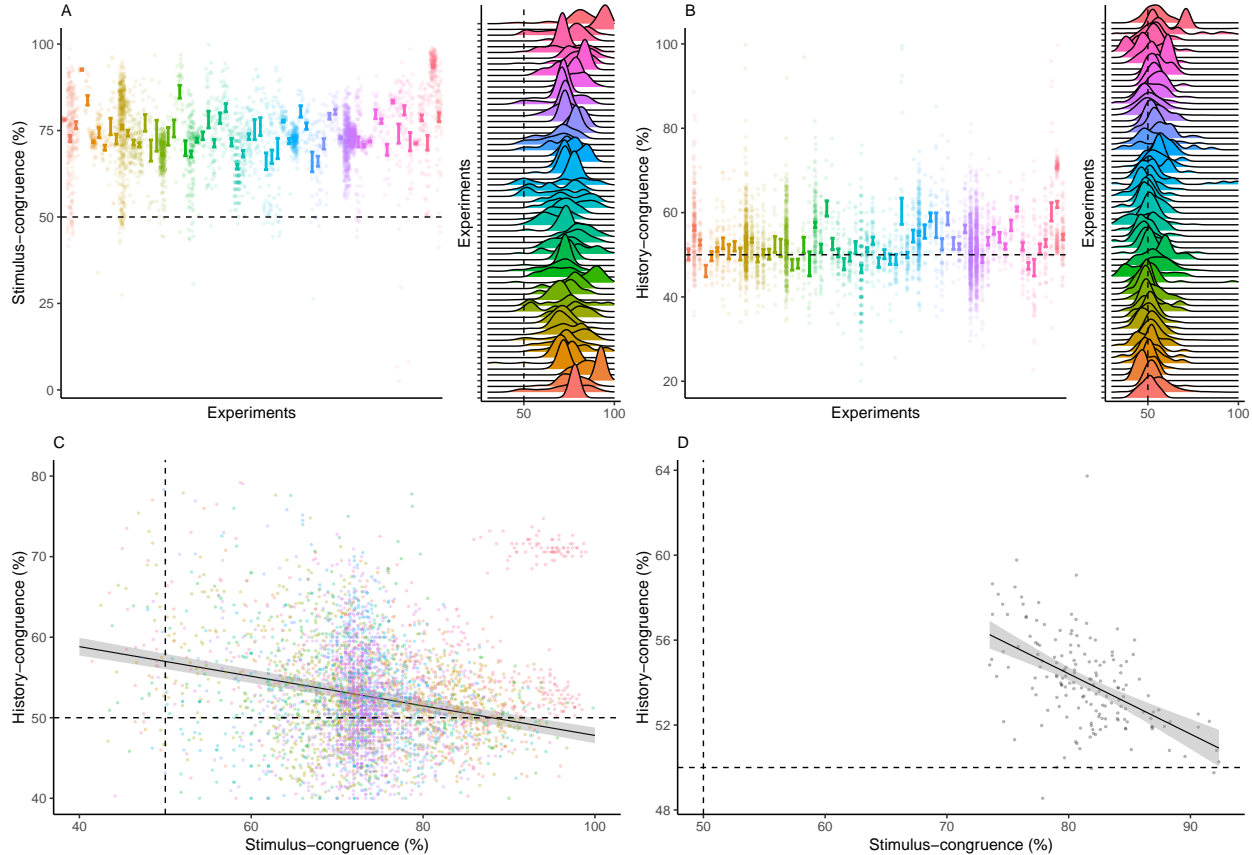
⁴ Department of Psychiatry (UPK), University of Basel, Switzerland

Corresponding Author:

Veith Weilnhammer, Helen Wills Neuroscience Institute, University of California Berkeley, USA, email: veith.weilnhammer@gmail.com

Supplemental Figures

0.1 Supplemental Figure S1



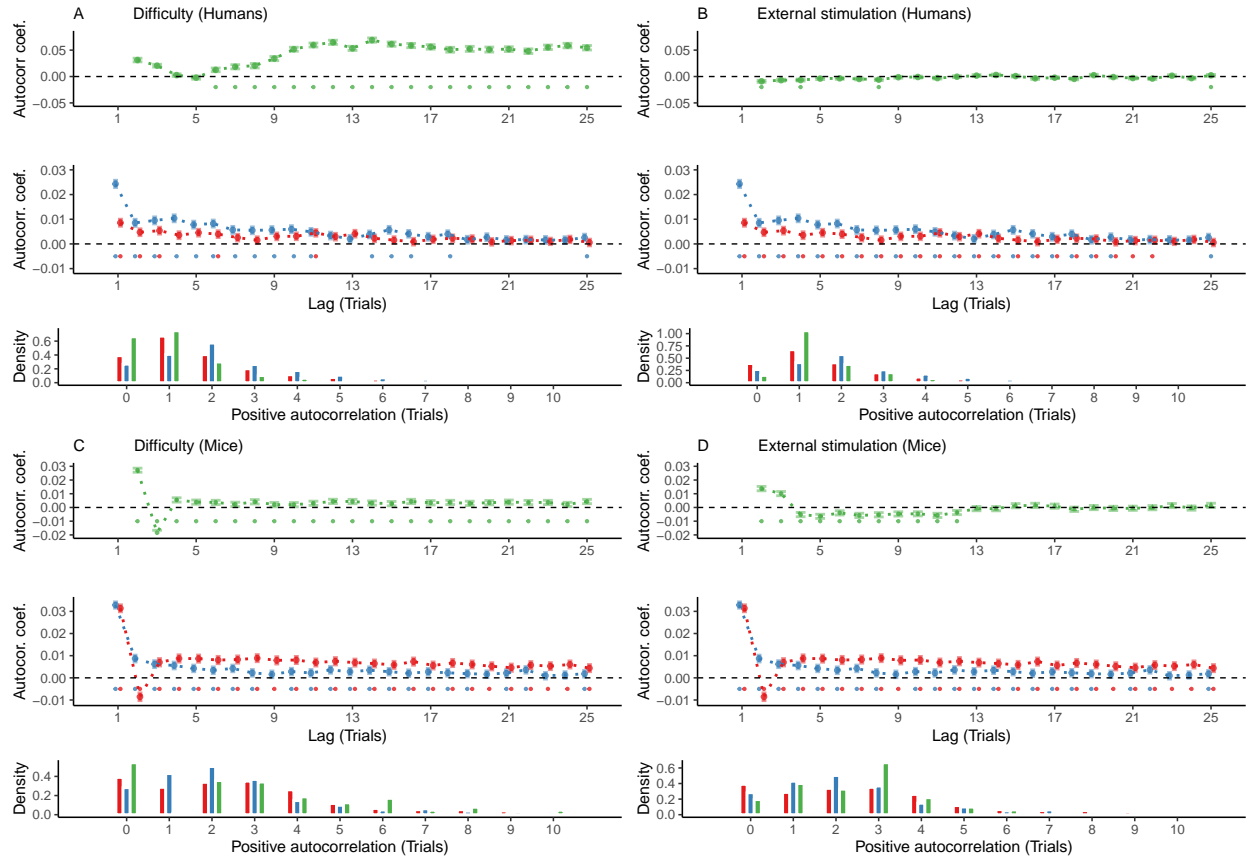
Supplemental Figure S1. Stimulus- and history-congruence.

- A. Stimulus-congruent choices in humans amounted to $73.46\% \pm 0.15\%$ of trials and were highly consistent across the experiments selected from the Confidence Database.
- B. History-congruent choices in humans amounted to $52.7\% \pm 0.12\%$ of trials. In analogy to stimulus-congruence, the prevalence of history-congruence was highly consistent across the experiments selected from the Confidence Database. 48.48% of experiments showed significant ($p < 0.05$) biases toward preceding choices, whereas 2 of the 66 of the included experiments showed significant repelling biases.
- C. In humans, we found an enhanced impact of perceptual history in participants who were

less sensitive to external sensory information ($T(4.3 \times 10^3) = -14.27$, $p = 3.78 \times 10^{-45}$), suggesting that perception results from the competition of external with internal information.

D. In analogy to humans, mice that were less sensitive to external sensory information showed stronger biases toward perceptual history ($T(163) = -7.52$, $p = 3.44 \times 10^{-12}$, Pearson correlation).

0.2 Supplemental Figure S2



Supplemental Figure S2. Controlling for task difficulty and external stimulation.

In this study, we found highly significant autocorrelations of stimulus- and history-congruence in humans as well as in mice, while controlling for task difficulty and the sequence of external stimulation. Here, we confirm that the autocorrelations of stimulus- and history-congruence were not a trivial consequence of the experimental design or the addition of tast difficulty and external stimulation as control variables in the computation of group-level autocorrelations.

A. In humans, task difficulty (in green) showed a significant autocorrelation starting at the 5th trial (upper panel, dots at the bottom indicate intercepts $\neq 0$ in trial-wise linear mixed effects modeling at $p < 0.05$). When controlling for task difficulty only, linear mixed effects modeling indicated a significant autocorrelation of stimulus-congruence (in red) for the first 3 consecutive trials (middle panel). 20% of trials within the displayed time window remained significantly autocorrelated. The autocorrelation of history-congruence (in blue) remained

significant for the first 11 consecutive trials (64% significantly autocorrelated trials within the displayed time window). At the level of individual participants, the autocorrelation of task difficulty exceeded the respective autocorrelation of randomly permuted within a lag of $21.66 \pm 8.37 \times 10^{-3}$ trials (lower panel).

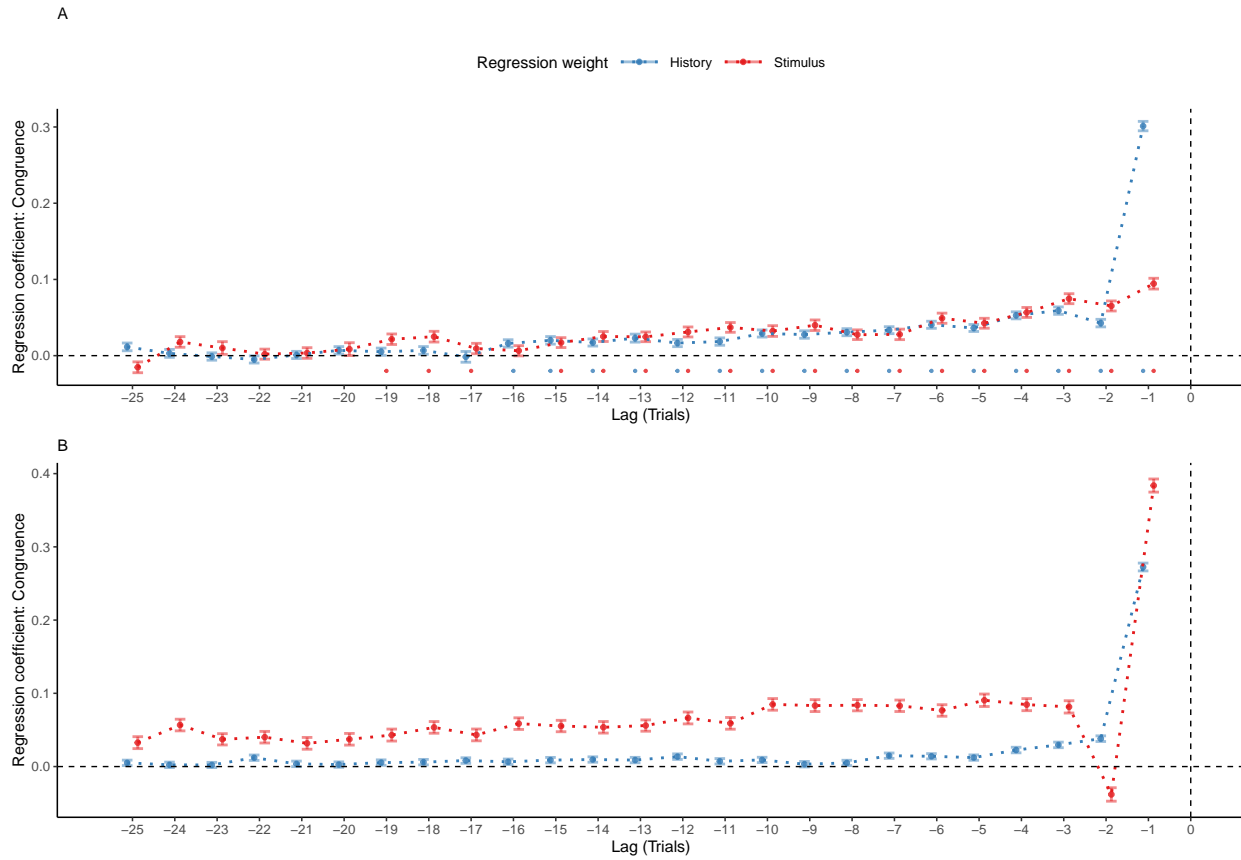
B. In humans, the sequence of external stimulation (i.e., which of the two binary outcomes was supported by the presented stimuli; depicted in green) was negatively autocorrelated for 1 trial. When controlling for the autocorrelation of external stimulation only, stimulus-congruence remained significantly autocorrelated for 22 consecutive trials (88% of trials within the displayed time window; lower panel) and history-congruence remained significantly autocorrelated for 20 consecutive trials (84% of trials within the displayed time window). At the level of individual participants, the autocorrelation of external stimulation exceeded the respective autocorrelation of randomly permuted within a lag of $2.94 \pm 4.4 \times 10^{-3}$ consecutive trials (lower panel).

C. In mice, task difficulty showed a significant autocorrelated for the first 25 consecutive trials (upper panel). When controlling only for task difficulty only, linear mixed effects modeling indicated a significant autocorrelation of stimulus-congruence for the first 36 consecutive trials (middle panel). In total, 100% of trials within the displayed time window remained significantly autocorrelated. The autocorrelation of history-congruence remained significant for the first 8 consecutive trials, with 84% significantly autocorrelated trials within the displayed time window. At the level of individual mice, autocorrelation coefficients for difficulty were elevated above randomly permuted data within a lag of 15.13 ± 0.19 consecutive trials (lower panel).

D. In mice, the sequence of external stimulation (i.e., which of the two binary outcomes was supported by the presented stimuli) was negatively autocorrelated for 11 consecutive trials (upper panel). When controlling only for the autocorrelation of external stimulation, stimulus-congruence remained significantly autocorrelated for 86 consecutive trials (100% of trials within the displayed time window; middle) and history-congruence remained significantly

autocorrelated for 8 consecutive trials (84% of trials within the displayed time window). At the level of individual mice, autocorrelation coefficients for external stimulation were elevated above randomly permuted data within a lag of $2.53 \pm 9.8 \times 10^{-3}$ consecutive trials (lower panel).

0.3 Supplemental Figure S3



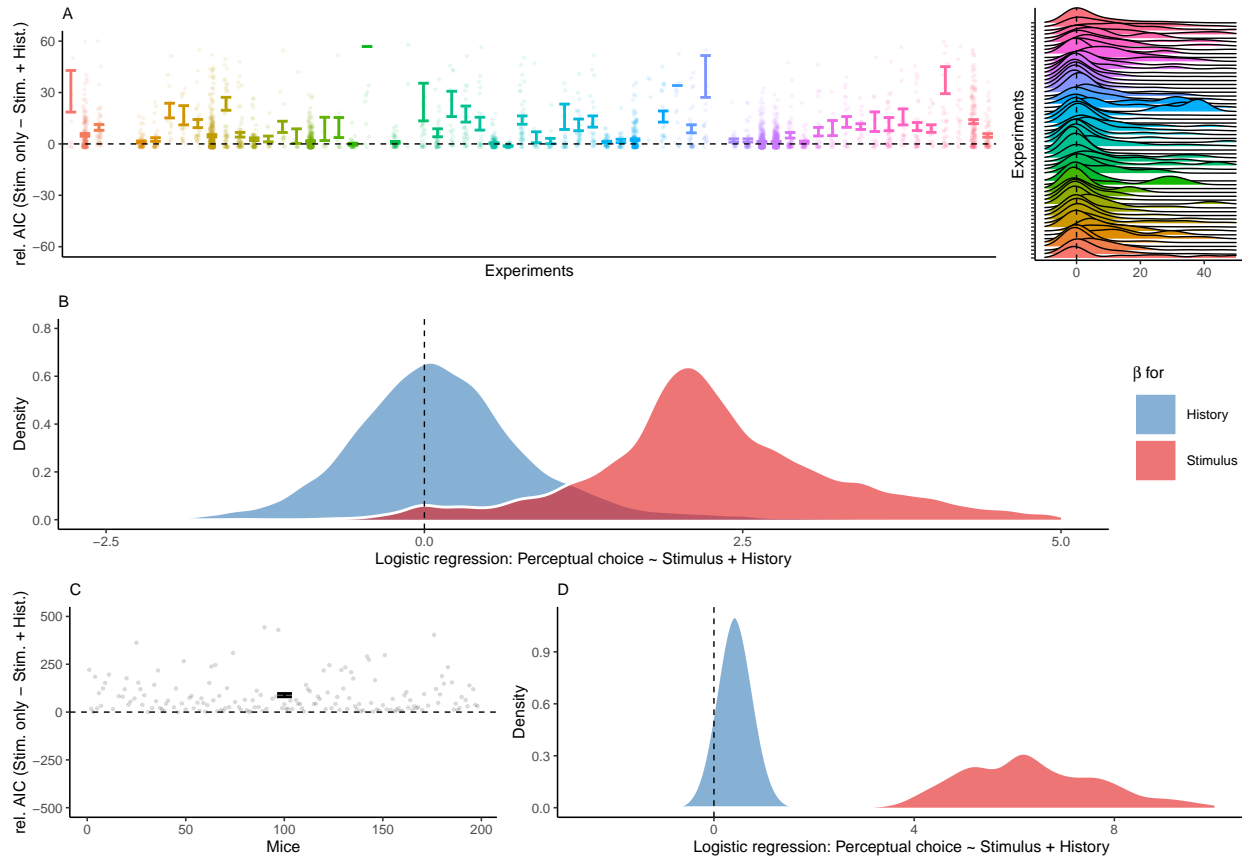
Supplemental Figure S3. Reproducing group-level autocorrelations using logistic regression.

A. As an alternative to group-level autocorrelation coefficients, we used trial-wise logistic regression to quantify serial dependencies in stimulus- and history-congruence. This analysis predicted stimulus- and history-congruence at the index trial (trial $t = 0$, vertical line) based on stimulus- and history-congruence at the 100 preceding trials. Mirroring the shape of the group-level autocorrelations, trial-wise regression coefficients (depicted as mean \pm SEM, dots mark trials with regression weights significantly greater than zero at $p < 0.05$) increased toward the index trial $t = 0$ for the human data.

B. Following our results in human data, regression coefficients that predicted history-congruence at the index trial (trial $t = 0$, vertical line) increased exponentially for trials closer to the index trial in mice. In contrast to history-congruence, stimulus-congruence

showed a negative regression weight (or autocorrelation coefficient; Figure 3B) at trial -2. This was due to the experimental design (see also the autocorrelations of difficulty and external stimulation in Supplemental Figure S2C and D): When mice made errors at easy trials (contrast $\geq 50\%$), the upcoming stimulus was shown at the same spatial location and at high contrast. This increased the probability of stimulus-congruent perceptual choices after stimulus-incongruent perceptual choices at easy trials, thereby creating a negative regression weight (or autocorrelation coefficient) of stimulus-congruence at trial -2.

0.4 Supplemental Figure S4



Supplemental Figure S4. History-congruence in logistic regression.

A. To ensure that perceptual history played a significant role in perception despite the ongoing stream of external information, we tested whether human perceptual decision-making was better explained by the combination of external and internal information or, alternatively, by external information alone. To this end, we compared AIC between logistic regression models that predicted trial-wise perceptual responses either by both current external sensory information and the preceding percept, or by external sensory information alone (values above zero indicate a superiority of the full model). With high consistency across the experiments selected from the Confidence Database, this model-comparison confirmed that perceptual history contributed significantly to perception (difference in AIC = 8.07 ± 0.53 , $T(57.22) = 4.1$, $p = 1.31 \times 10^{-4}$).

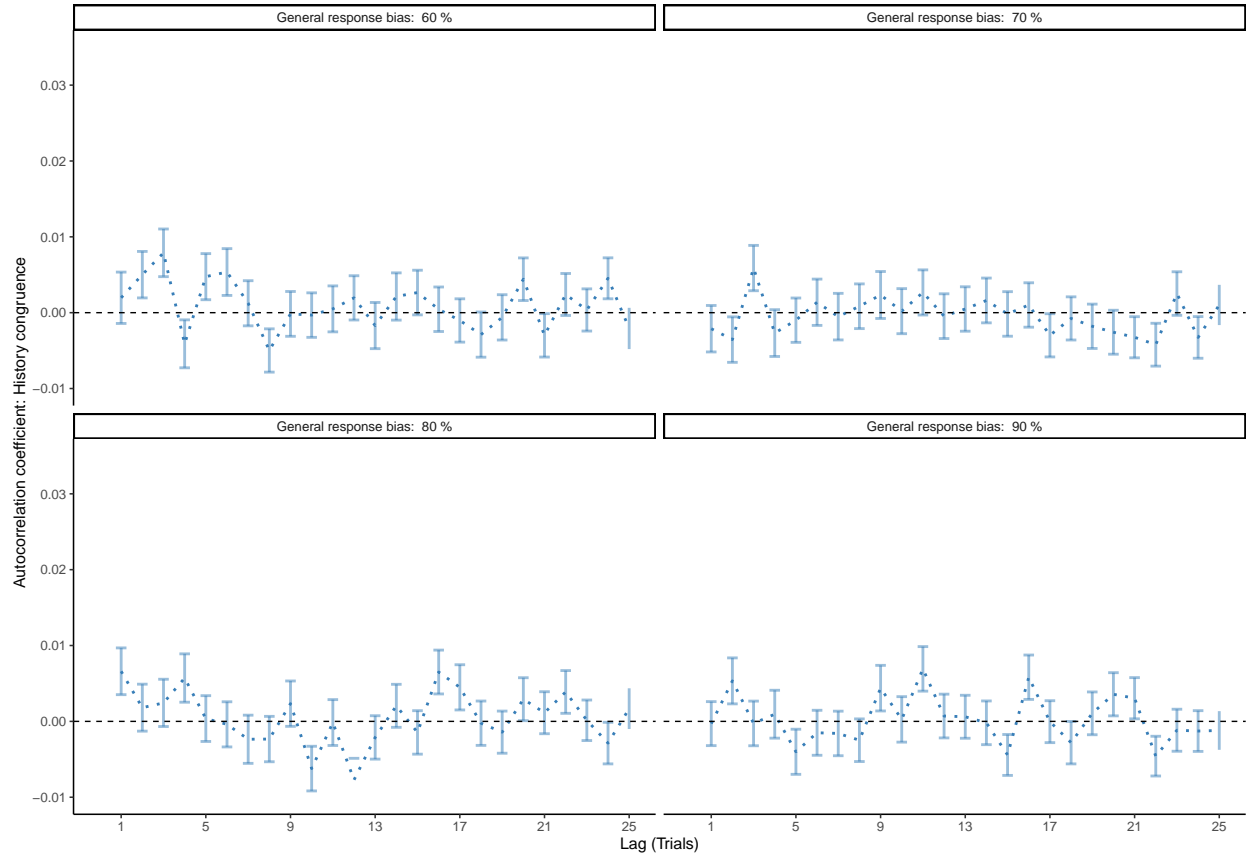
B. Participant-wise regression coefficients amount to 0.18 ± 0.02 for the effect of perceptual

history and 2.51 ± 0.03 for external sensory stimulation.

C. In mice, an AIC-based model comparison indicated that perception was better explained by logistic regression models that predicted trial-wise perceptual responses based on both current external sensory information and the preceding percept (difference in AIC = 88.62 ± 8.57 , $T(164) = -10.34$, $p = 1.29 \times 10^{-19}$).

D. In mice, individual regression coefficients amounted to 0.42 ± 0.02 for the effect of perceptual history and 6.91 ± 0.21 for external sensory stimulation.

0.5 Supplemental Figure S5

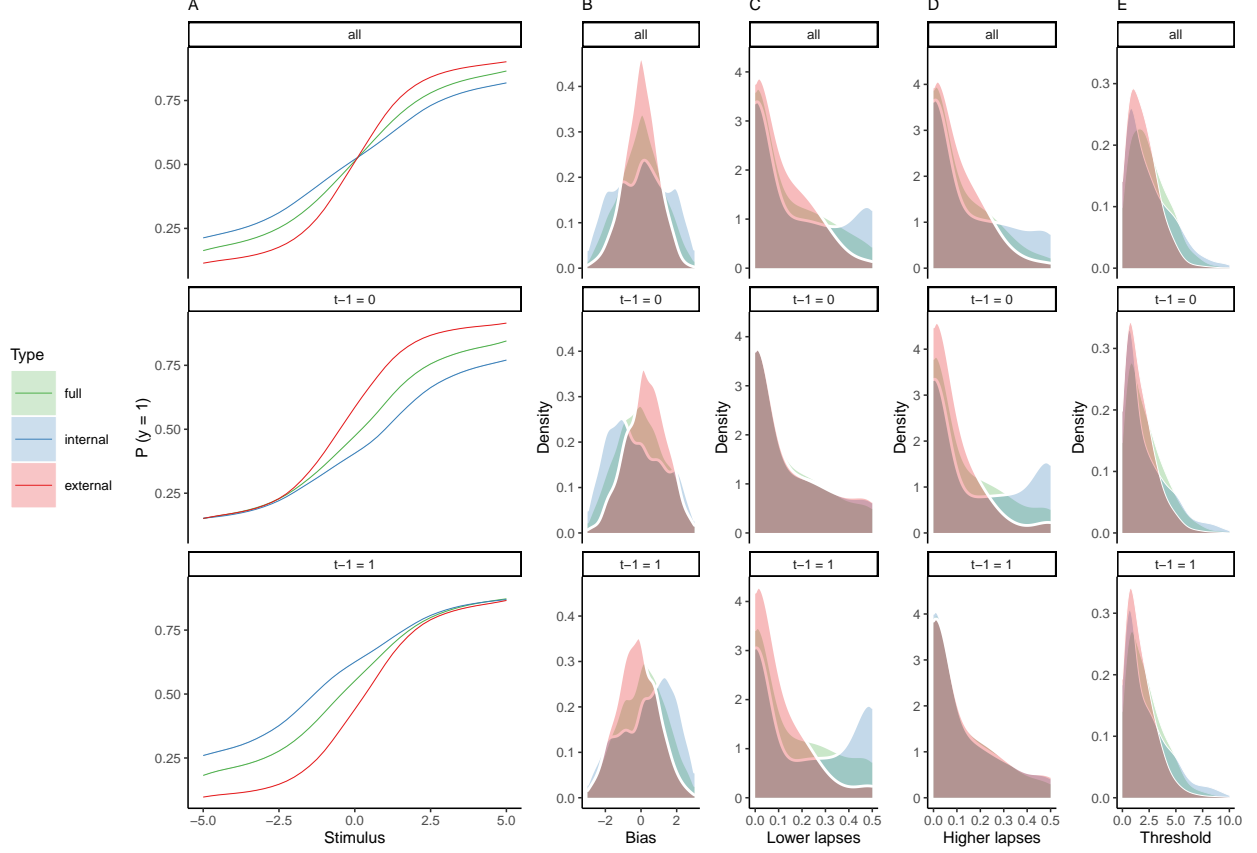


Supplemental Figure S5. Correcting for general response biases.

Here, we ask whether the autocorrelation of history-congruence (as shown in Figure 2-3C) may be driven by general response biases (i.e., a general propensity to choose one of the two possible outcomes more frequently than the alternative). To this end, we generated sequences of 100 perceptual choices with general response biases ranging from 60 to 90% for 1000 simulated participants each. We then computed the autocorrelation of history-congruence for these simulated data. Crucially, we used the correction procedure that is applied to the autocorrelation curves shown in this manuscript: All reported autocorrelation coefficients are computed relative to the average autocorrelation coefficients obtained for 100 iterations of randomly permuted trial sequences. The above simulation show that this correction procedure removes any potential contribution of general response biases to the autocorrelation of history-congruence. This indicates that the autocorrelation of history-congruence (as shown in Figure

2-3C) is not driven by general response biases that were present in the empirical data at a level of $58.71\% \pm 0.22\%$ in humans and $54.6\% \pm 0.3\%$ in mice.

0.6 Supplemental Figure S6



Supplemental Figure S6. Full and history-conditioned psychometric functions across modes in humans.

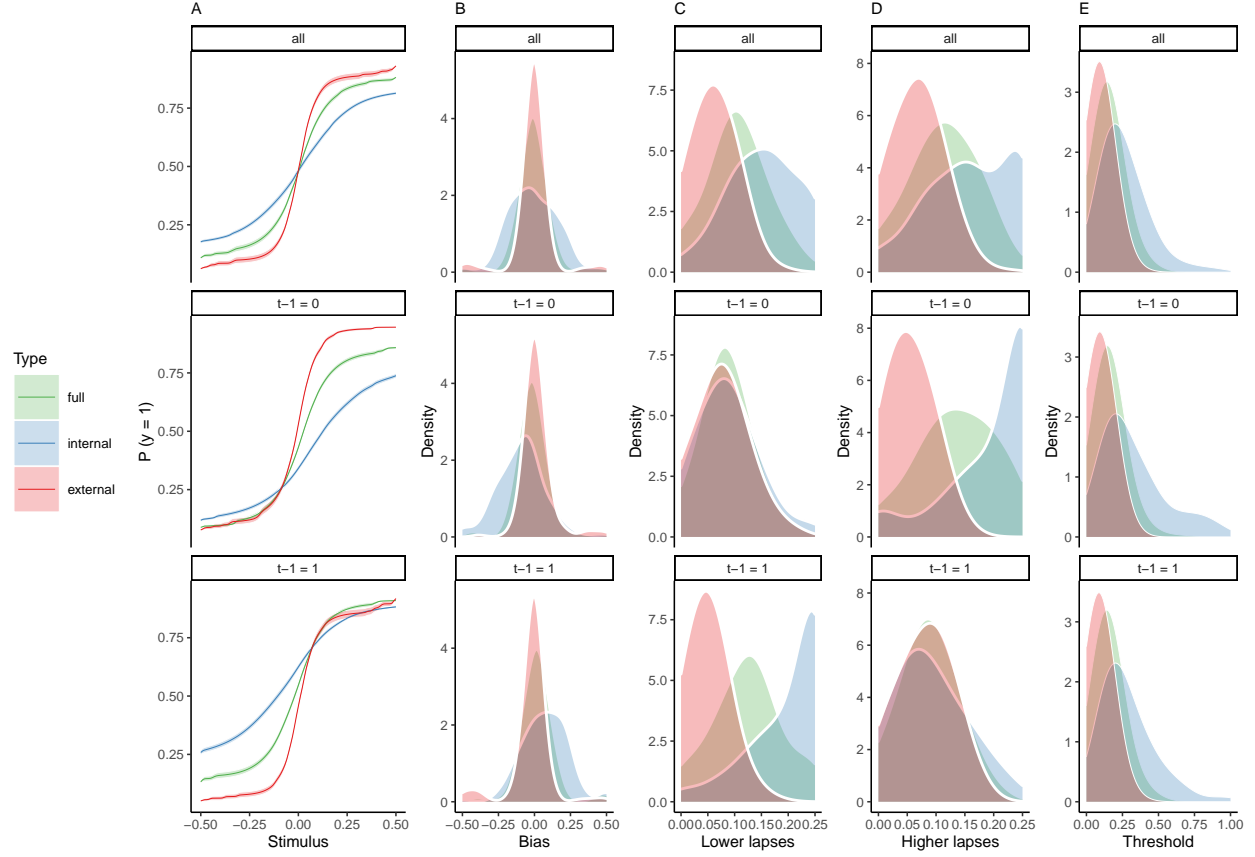
- A. Here, we show average psychometric functions for the full dataset (upper panel) and conditioned on perceptual history ($y_{t-1} = 1$ and $y_{t-1} = 0$; middle and lower panel) across modes (green line) and for internal mode (blue line) and external mode (red line) separately.
- B. Across the full dataset, biases μ were distributed around zero ($\beta_0 = 7.37 \times 10^{-3} \pm 0.09$, $T(36.8) = 0.08$, $p = 0.94$; upper panel), with larger absolute biases $|\mu|$ for internal as compared to external mode ($\beta_0 = -0.62 \pm 0.07$, $T(45.62) = -8.38$, $p = 8.59 \times 10^{-11}$; controlling for differences in lapses and thresholds). When conditioned on perceptual history, we observed negative biases for $y_{t-1} = 0$ ($\beta_0 = 0.56 \pm 0.12$, $T(43.39) = 4.6$, $p = 3.64 \times 10^{-5}$; middle panel) and positive biases for $y_{t-1} = 1$ ($\beta_0 = 0.56 \pm 0.12$, $T(43.39) = 4.6$, $p = 3.64 \times 10^{-5}$; lower panel).

C. Lapse rates were higher in internal mode as compared to external mode ($\beta_0 = -0.05 \pm 5.73 \times 10^{-3}$, $T(47.03) = -9.11$, $p = 5.94 \times 10^{-12}$; controlling for differences in biases and thresholds; see upper panel and subplot D). Importantly, the between-mode difference in lapses depended on perceptual history: We found no significant difference in lower lapses γ for $y_{t-1} = 0$ ($\beta_0 = 0.01 \pm 7.77 \times 10^{-3}$, $T(33.1) = 1.61$, $p = 0.12$; middle panel), but a significant difference for $y_{t-1} = 1$ ($\beta_0 = -0.11 \pm 0.01$, $T(40.11) = -9.59$, $p = 6.14 \times 10^{-12}$; lower panel).

D. Conversely, higher lapses δ were significantly increased for $y_{t-1} = 0$ ($\beta_0 = -0.1 \pm 9.58 \times 10^{-3}$, $T(36.87) = -10.16$, $p = 3.06 \times 10^{-12}$; middle panel), but not for $y_{t-1} = 1$ ($\beta_0 = 0.01 \pm 7.74 \times 10^{-3}$, $T(33.66) = 1.58$, $p = 0.12$; lower panel).

E. The thresholds t were larger in internal as compared to external mode ($\beta_0 = -1.77 \pm 0.25$, $T(50.45) = -7.14$, $p = 3.48 \times 10^{-9}$; controlling for differences in biases and lapses) and were not modulated by perceptual history ($\beta_0 = 0.04 \pm 0.06$, $T(2.97 \times 10^3) = 0.73$, $p = 0.47$).

0.7 Supplemental Figure S7



Supplemental Figure S7. Full and history-conditioned psychometric functions across modes in mice.

A. Here, we show average psychometric functions for the full IBL dataset (upper panel) and conditioned on perceptual history ($y_{t-1} = 1$ and $y_{t-1} = 0$; middle and lower panel) across modes (green line) and for internal mode (blue line) and external mode (red line) separately.

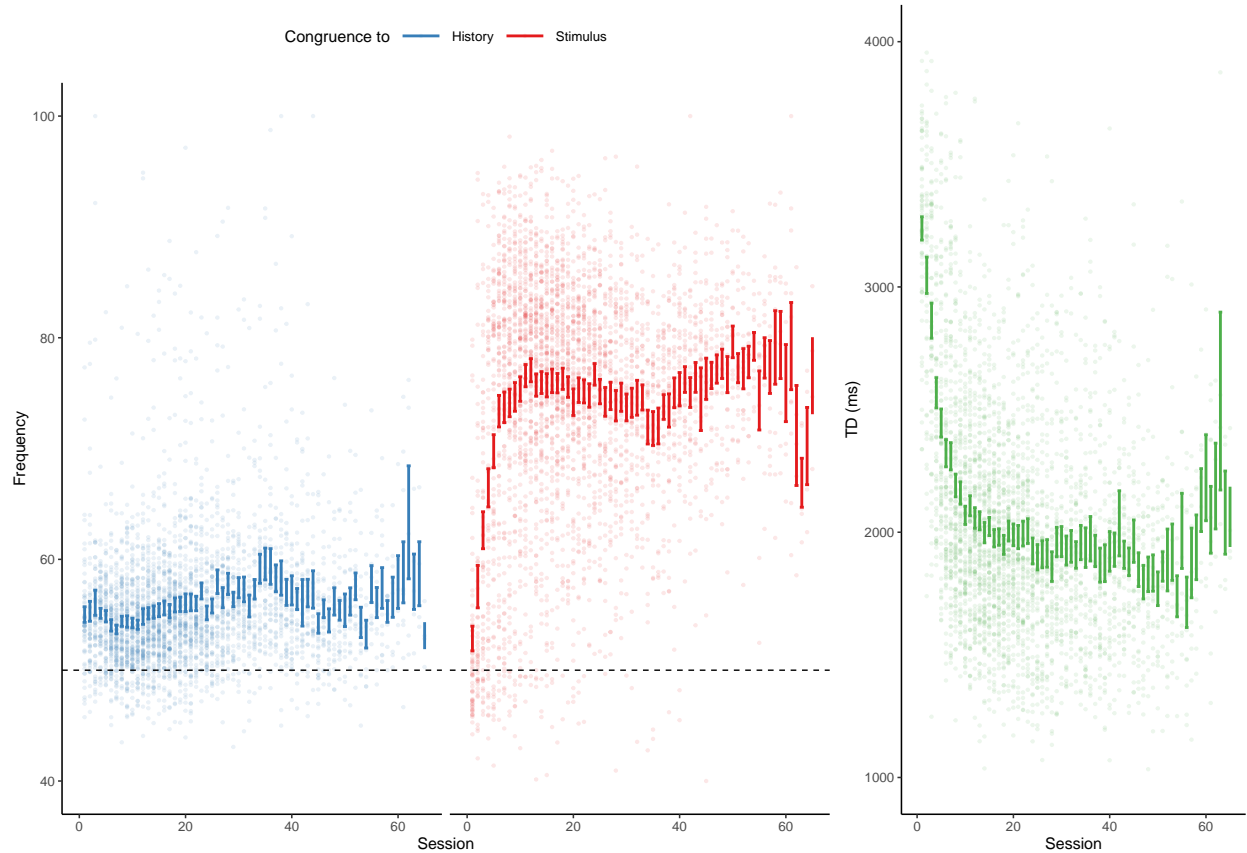
B. Across the full dataset, biases μ were distributed around zero ($T(164) = 0.39$, $p = 0.69$; upper panel), with larger absolute biases $|\mu|$ for internal as compared to external mode ($\beta_0 = -0.18 \pm 0.03$, $T = -6.38$, $p = 1.77 \times 10^{-9}$; controlling for differences in lapses and thresholds). When conditioned on perceptual history, we observed negative biases for $y_{t-1} = 0$ ($T(164) = -1.99$, $p = 0.05$; middle panel) and positive biases for $y_{t-1} = 1$ ($T(164) = 1.91$, $p = 0.06$; lower panel).

C. Lapse rates were higher in internal as compared to external mode ($\beta_0 = -0.11 \pm 4.39 \times 10^{-3}$, $T = -24.8$, $p = 4.91 \times 10^{-57}$; controlling for differences in biases and thresholds; upper panel, see subplot D). For $y_{t-1} = 1$, the difference between internal and external mode was more pronounced for lower lapses γ ($T(164) = -18.24$, $p = 2.68 \times 10^{-41}$) as compared to higher lapses δ (see subplot D). In mice, lower lapses γ were significantly elevated during internal mode irrespective of the preceding perceptual choice (middle panel: lower lapses γ for $y_{t-1} = 0$; $T(164) = -2.5$, $p = 0.01$, lower panel: lower lapses γ for $y_{t-1} = 1$; $T(164) = -32.44$, $p = 2.92 \times 10^{-73}$).

D. For $y_{t-1} = 0$, the difference between internal and external mode was more pronounced for higher lapses δ ($T(164) = 21.44$, $p = 1.93 \times 10^{-49}$, see subplot C). Higher lapses were significantly elevated during internal mode irrespective of the preceding perceptual choice (middle panel: higher lapses δ for $y_{t-1} = 0$; $T(164) = -28.29$, $p = 5.62 \times 10^{-65}$ lower panel: higher lapses δ for $y_{t-1} = 1$; $T(164) = -2.65$, $p = 8.91 \times 10^{-3}$).

E. Thresholds t were higher in internal as compared to external mode ($\beta_0 = -0.28 \pm 0.04$, $T = -7.26$, $p = 1.53 \times 10^{-11}$; controlling for differences in biases and lapses) and were not modulated by perceptual history ($T(164) = 0.94$, $p = 0.35$).

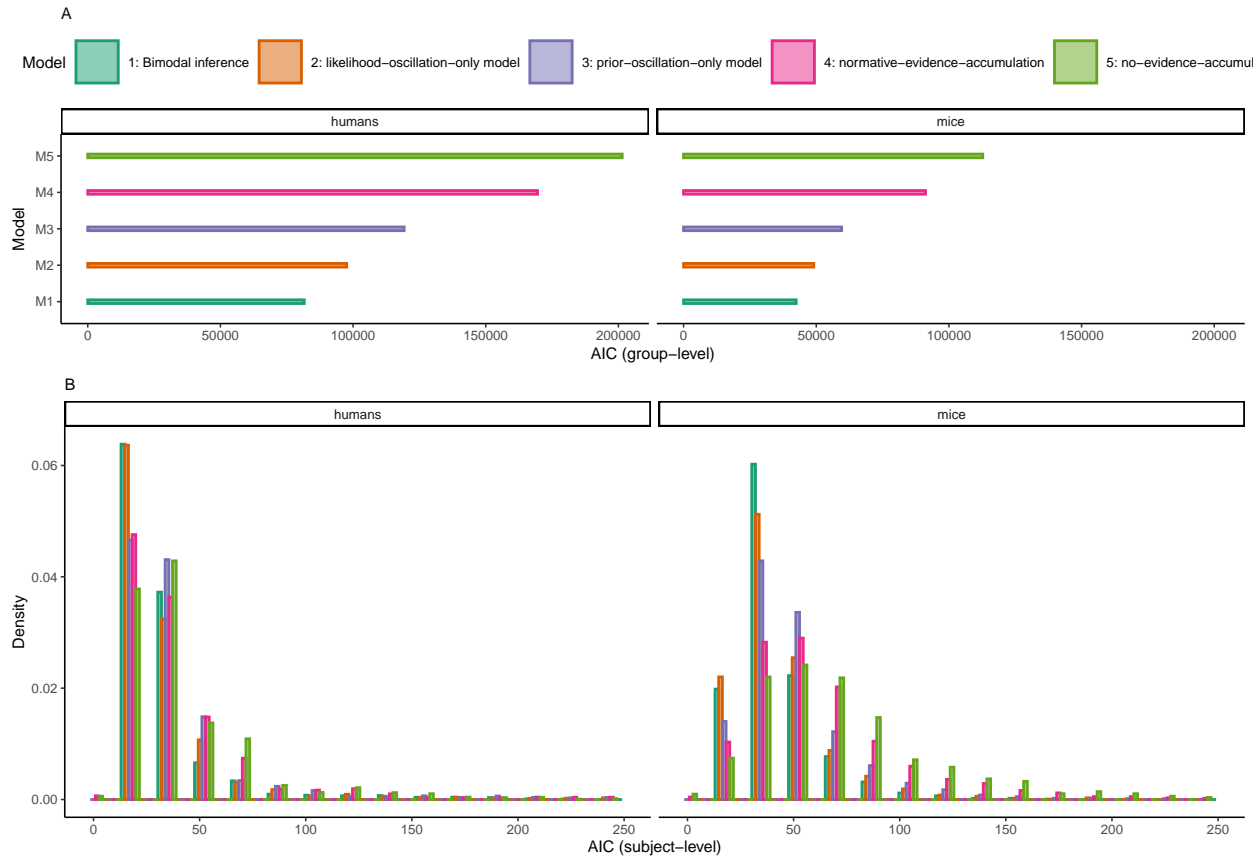
0.8 Supplemental Figure S8



Supplemental Figure S8. History-/stimulus-congruence and TDs during training of the basic task.

Here, we depict the progression of history- and stimulus-congruence (depicted in blue and red, respectively; left panel) as well as TDs (in green; right panel) across training sessions in mice that achieved proficiency (i.e., stimulus-congruence $\geq 80\%$) in the *basic* task of the IBL dataset. We found that both history-congruent perceptual choices ($\beta = 0.13 \pm 4.67 \times 10^{-3}$, $T(8.4 \times 10^3) = 27.04$, $p = 1.96 \times 10^{-154}$) and stimulus-congruent perceptual choices ($\beta = 0.34 \pm 7.13 \times 10^{-3}$, $T(8.51 \times 10^3) = 47.66$, $p < 2.2 \times 10^{-308}$) became more frequent with training. As in humans, mice showed shorter TDs with increased exposure to the task ($\beta = -22.14 \pm 17.06$, $T(1.14 \times 10^3) = -1.3$, $p < 2.2 \times 10^{-308}$).

0.9 Supplemental Figure S9



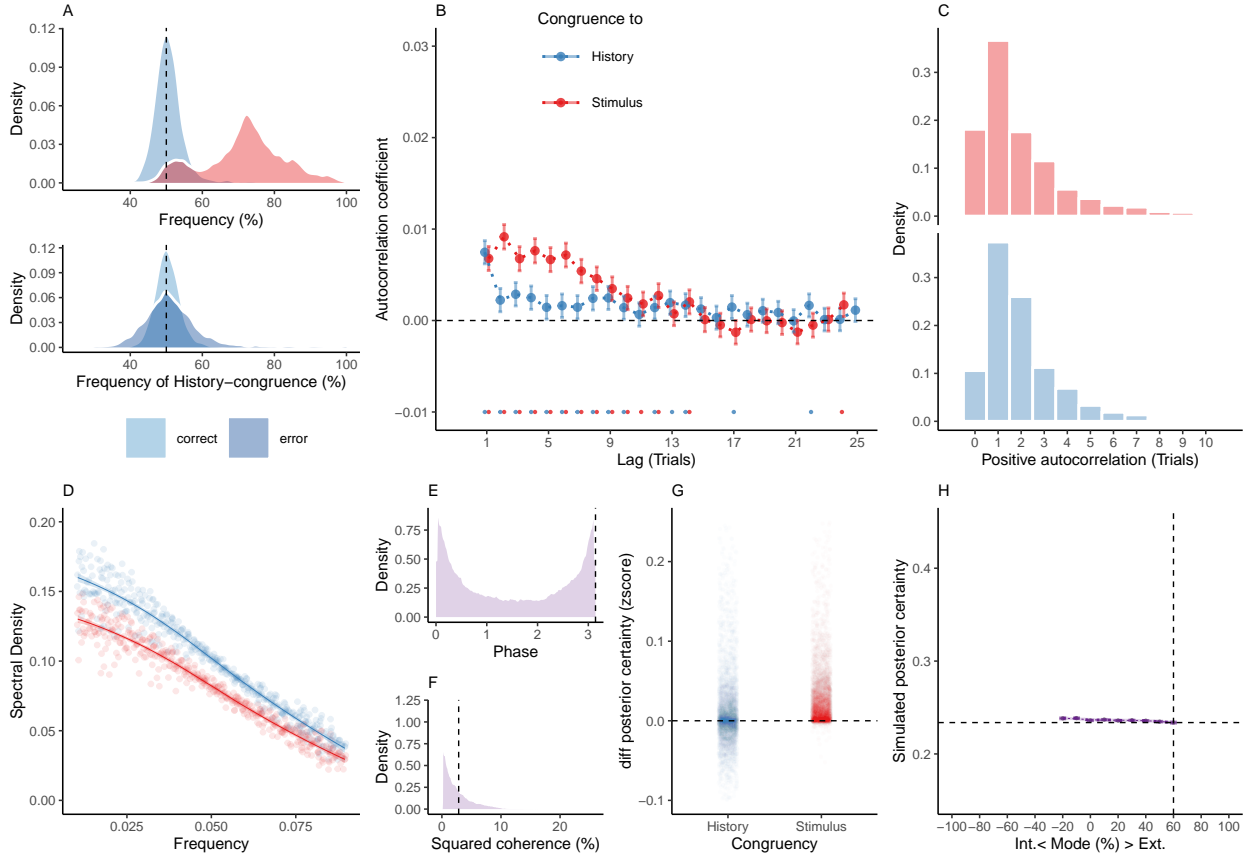
Supplemental Figure S9. Comparison of the bimodal inference model against reduced control models.

A. Group-level AIC. The bimodal inference model (M1) achieved the lowest AIC across the full model space ($AIC_1 = 8.16 \times 10^4$ in humans and 4.24×10^4 in mice). Model M2 ($AIC_2 = 9.76 \times 10^4$ in humans and 4.91×10^4 in mice) and Model M3 ($AIC_3 = 1.19 \times 10^5$ in humans and 5.95×10^4 in mice) incorporated only oscillations of either likelihood or prior precision. Model M4 ($AIC_4 = 1.69 \times 10^5$ in humans and 9.12×10^4 in mice) lacked any oscillations of likelihood and prior precision and corresponded to the normative model proposed by Glaze et al.⁵¹. In model M5 ($AIC_4 = 2.01 \times 10^5$ in humans and 1.13×10^5 in mice), we furthermore removed the integration of information across trials, such that perception depended only in incoming sensory information.

B. Subject-level AIC. Here, we show the distribution of AIC values at the subject-level.

AIC for the bimodal inference model tended to be smaller than AIC for the comparator models (statistical comparison to the second-best model M2 in humans: $\beta = -1.71 \pm 0.19$, $T(8.57 \times 10^3) = -8.85$, $p = 1.06 \times 10^{-18}$; mice: $T(1.57 \times 10^3) = -3.08$, $p = 2.12 \times 10^{-3}$).

0.10 Supplemental Figure S10



Supplemental Figure S10. Reduced Control Model M2: Only oscillation of the likelihood. When simulating data for the *likelihood-oscillation-only model*, we removed the oscillation from the prior term by setting the amplitude a_ψ to zero. Simulated data thus depended only on the participant-wise estimates for hazard rate H , amplitude a_{LLR} , frequency f , phase p and inverse decision temperature ζ .

A. Similar to the full model M1 (Figure 1F and Figure 4), simulated perceptual choices were stimulus-congruent in $71.97\% \pm 0.17\%$ of trials (in red). History-congruent amounted to $50.76\% \pm 0.07\%$ of trials (in blue). As in the full model, the likelihood-oscillation-only model showed a significant bias toward perceptual history $T(4.32 \times 10^3) = 10.29$, $p = 1.54 \times 10^{-24}$; upper panel). Similarly, history-congruent choices were more frequent at error trials ($T(4.32 \times 10^3) = 9.71$, $p = 4.6 \times 10^{-22}$; lower panel).

B. In the likelihood-oscillation-only model, we observed that the autocorrelation coefficients for

history-congruence were reduced below the autocorrelation coefficients of stimulus-congruence. This is an approximately five-fold reduction relative to the empirical results observed in humans (Figure 2B), where the autocorrelation of history-congruence was above the autocorrelation of stimulus-congruence. Moreover, in the reduced model shown here, the number of consecutive trials that showed significant autocorrelation of history-congruence was reduced to 11.

C. In the likelihood-oscillation-only model, the number of consecutive trials at which true autocorrelation coefficients exceeded the autocorrelation coefficients for randomly permuted data did not differ with respect to stimulus-congruence ($2.62 \pm 1.39 \times 10^{-3}$ trials; $T(4.32 \times 10^3) = 1.85$, $p = 0.06$), but decreased with respect to history-congruence ($2.4 \pm 8.45 \times 10^{-4}$ trials; $T(4.32 \times 10^3) = -15.26$, $p = 3.11 \times 10^{-51}$) relative to the full model.

D. In the likelihood-oscillation-only model, the smoothed probabilities of stimulus- and history-congruence (sliding windows of ± 5 trials) fluctuated as a scale-invariant process with a $1/f$ power law, i.e., at power densities that were inversely proportional to the frequency (power $\sim 1/f^\beta$; stimulus-congruence: $\beta = -0.81 \pm 1.17 \times 10^{-3}$, $T(1.92 \times 10^5) = -688.65$, $p < 2.2 \times 10^{-308}$; history-congruence: $\beta = -0.79 \pm 1.14 \times 10^{-3}$, $T(1.92 \times 10^5) = -698.13$, $p < 2.2 \times 10^{-308}$).

E. In the likelihood-oscillation-only model, the distribution of phase shift between fluctuations in simulated stimulus- and history-congruence peaked at half a cycle (π denoted by dotted line). In contrast to the full model, the dynamic probabilities of simulated stimulus- and history-congruence were positively correlated ($\beta = 2.7 \times 10^{-3} \pm 7.6 \times 10^{-4}$, $T(2.02 \times 10^6) = 3.55$, $p = 3.8 \times 10^{-4}$).

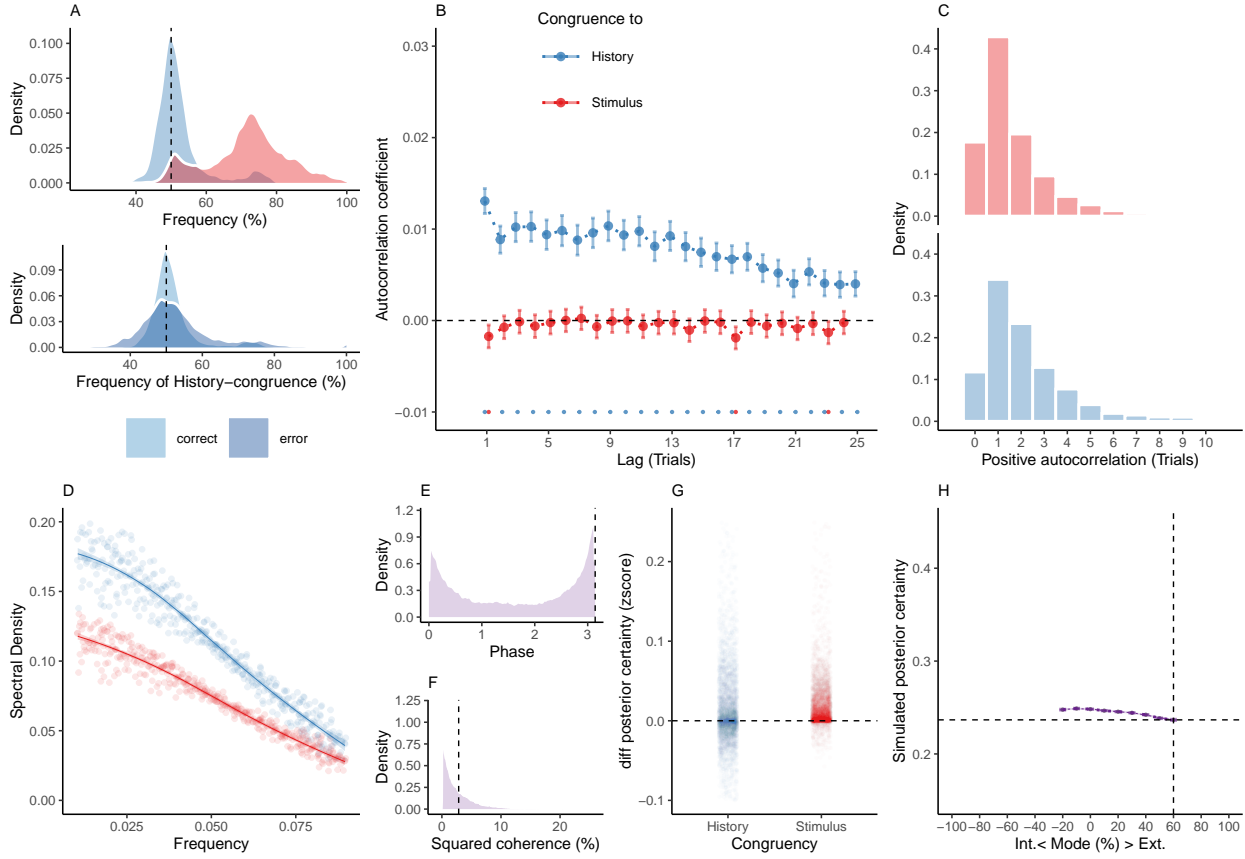
F. In the likelihood-oscillation-only model, the average squared coherence between fluctuations in simulated stimulus- and history-congruence (black dotted line) was reduced in comparison to the full model ($T(3.51 \times 10^3) = -4.56$, $p = 5.27 \times 10^{-6}$) and amounted to $3.43 \pm 1.02 \times 10^{-3}\%$.

G. Similar to the full bimodal inference model, confidence simulated from the likelihood-oscillation-only model was enhanced for stimulus-congruent choices ($\beta = 0.03 \pm 1.42 \times 10^{-4}$,

$T(2.1 \times 10^6) = 191.78$, $p < 2.2 \times 10^{-308}$) and history-congruent choices ($\beta = 9.1 \times 10^{-3} \pm 1.25 \times 10^{-4}$, $T(2.1 \times 10^6) = 72.51$, $p < 2.2 \times 10^{-308}$).

H. In the likelihood-oscillation-only model, the positive quadratic relationship between the mode of perceptual processing and confidence was markedly reduced in comparison to the full model ($\beta_2 = 0.34 \pm 0.1$, $T(2.1 \times 10^6) = 3.49$, $p = 4.78 \times 10^{-4}$). The horizontal and vertical dotted lines indicate minimum posterior certainty and the associated mode, respectively.

0.11 Supplemental Figure S11



Supplemental Figure S11. Reduced Control Model M3: Only oscillation of the prior. When simulating data for the *prior-oscillation-only model*, we removed the oscillation from the prior term by setting the amplitude a_{LLR} to zero. Simulated data thus depended only on the participant-wise estimates for hazard rate H , amplitude a_ψ , frequency f , phase p and inverse decision temperature ζ .

A. Similar to the full model (Figure 1F and Figure 4), simulated perceptual choices were stimulus-congruent in $71.97\% \pm 0.17\%$ of trials (in red). History-congruent amounted to $52.1\% \pm 0.11\%$ of trials (in blue). As in the full model, the prior-oscillation-only showed a significant bias toward perceptual history $T(4.32 \times 10^3) = 18.34$, $p = 1.98 \times 10^{-72}$; upper panel). Similarly, history-congruent choices were more frequent at error trials ($T(4.31 \times 10^3) = 12.35$, $p = 1.88 \times 10^{-34}$; lower panel).

B. In the prior-oscillation-only model, we did not observe any significant positive autocor-

relation of stimulus-congruence , whereas the autocorrelation of history-congruence was preserved.

C. In the prior-oscillation-only model, the number of consecutive trials at which true autocorrelation coefficients exceeded the autocorrelation coefficients for randomly permuted data did was decreased with respect to stimulus-congruence relative to the full model ($1.8 \pm 1.01 \times 10^{-3}$ trials; $T(4.31 \times 10^3) = -6.48$, $p = 1.03 \times 10^{-10}$), but did not differ from the full model with respect to history-congruence ($4.25 \pm 1.84 \times 10^{-3}$ trials; $T(4.32 \times 10^3) = 0.07$, $p = 0.95$).

D. In the prior-oscillation-only model, the smoothed probabilities of stimulus- and history-congruence (sliding windows of ± 5 trials) fluctuated as a scale-invariant process with a $1/f$ power law, i.e., at power densities that were inversely proportional to the frequency (power $\sim 1/f^\beta$; stimulus-congruence: $\beta = -0.78 \pm 1.11 \times 10^{-3}$, $T(1.92 \times 10^5) = -706.62$, $p < 2.2 \times 10^{-308}$; history-congruence: $\beta = -0.83 \pm 1.27 \times 10^{-3}$, $T(1.92 \times 10^5) = -651.6$, $p < 2.2 \times 10^{-308}$).

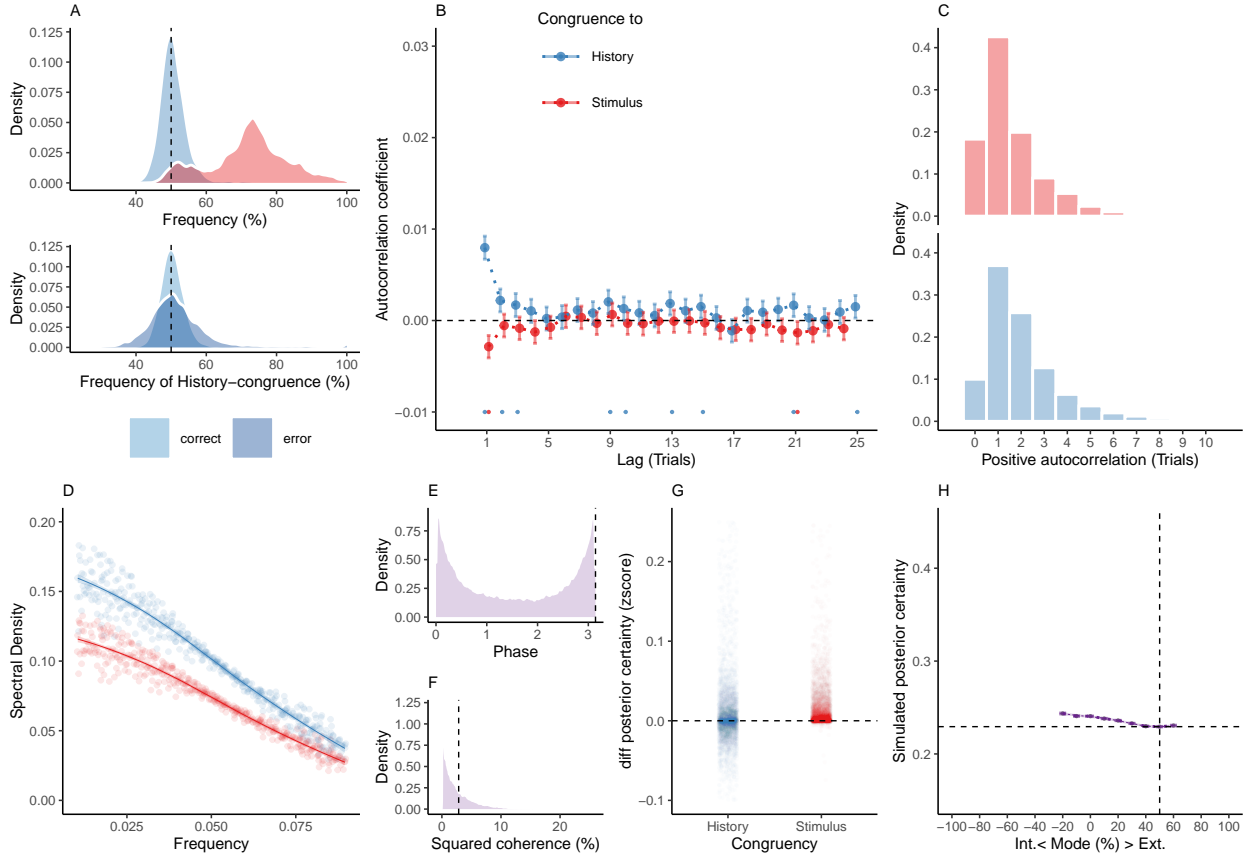
E. In the prior-oscillation-only model, the distribution of phase shift between fluctuations in simulated stimulus- and history-congruence peaked at half a cycle (π denoted by dotted line). Similar to the full model, the dynamic probabilities of simulated stimulus- and history-congruence were anti-correlated ($\beta = -0.03 \pm 8.61 \times 10^{-4}$, $T(2.12 \times 10^6) = -34.03$, $p = 8.17 \times 10^{-254}$).

F. In the prior-oscillation-only model, the average squared coherence between fluctuations in simulated stimulus- and history-congruence (black dotted line) was reduced in comparison to the full model ($T(3.54 \times 10^3) = -3.22$, $p = 1.28 \times 10^{-3}$) and amounted to $3.52 \pm 1.04 \times 10^{-3}\%$.

G. Similar to the full bimodal inference model, confidence simulated from the prior-oscillation-only model was enhanced for stimulus-congruent choices ($\beta = 0.02 \pm 1.44 \times 10^{-4}$, $T(2.03 \times 10^6) = 128.53$, $p < 2.2 \times 10^{-308}$) and history-congruent choices ($\beta = 0.01 \pm 1.26 \times 10^{-4}$, $T(2.03 \times 10^6) = 88.24$, $p < 2.2 \times 10^{-308}$).

H. In contrast to the full bimodal inference model, the prior-oscillation-only model did not yield a positive quadratic relationship between the mode of perceptual processing and confidence ($\beta_2 = -0.17 \pm 0.1$, $T(2.04 \times 10^6) = -1.66$, $p = 0.1$). The horizontal and vertical dotted lines indicate minimum posterior certainty and the associated mode, respectively.

0.12 Supplemental Figure S12



Supplemental Figure S12. Reduced Control Model M4: Normative evidence accumulation. When simulating data for the *normative-evidence-accumulation model*, we removed the oscillation from the likelihood and prior terms by setting the amplitudes a_{LLR} and a_ψ to zero. Simulated data thus depended only on the participant-wise estimates for hazard rate H and inverse decision temperature ζ .

A. Similar to the full model (Figure 1F and Figure 4), simulated perceptual choices were stimulus-congruent in $71.97\% \pm 0.17\%$ of trials (in red). History-congruent amounted to $50.73\% \pm 0.07\%$ of trials (in blue). As in the full model, the no-oscillation model showed a significant bias toward perceptual history $T(4.32 \times 10^3) = 9.94$, $p = 4.88 \times 10^{-23}$; upper panel). Similarly, history-congruent choices were more frequent at error trials ($T(4.31 \times 10^3) = 10.59$, $p = 7.02 \times 10^{-26}$; lower panel).

B. In the normative-evidence-accumulation model, we did not find significant autocor-

relations for stimulus-congruence. Likewise, we did not observe any autocorrelation of history-congruence beyond the first three consecutive trials.

C. In the normative-evidence-accumulation model, the number of consecutive trials at which true autocorrelation coefficients exceeded the autocorrelation coefficients for randomly permuted data decreased with respect to both stimulus-congruence ($1.8 \pm 1.59 \times 10^{-3}$ trials; $T(4.31 \times 10^3) = -5.21$, $p = 2 \times 10^{-7}$) and history-congruence ($2.18 \pm 5.48 \times 10^{-4}$ trials; $T(4.32 \times 10^3) = -17.1$, $p = 1.75 \times 10^{-63}$) relative to the full model.

D. In the normative-evidence-accumulation model, the smoothed probabilities of stimulus- and history-congruence (sliding windows of ± 5 trials) fluctuated as a scale-invariant process with a $1/f$ power law, i.e., at power densities that were inversely proportional to the frequency (power $\sim 1/f^\beta$; stimulus-congruence: $\beta = -0.78 \pm 1.1 \times 10^{-3}$, $T(1.92 \times 10^5) = -706.93$, $p < 2.2 \times 10^{-308}$; history-congruence: $\beta = -0.79 \pm 1.12 \times 10^{-3}$, $T(1.92 \times 10^5) = -702.46$, $p < 2.2 \times 10^{-308}$).

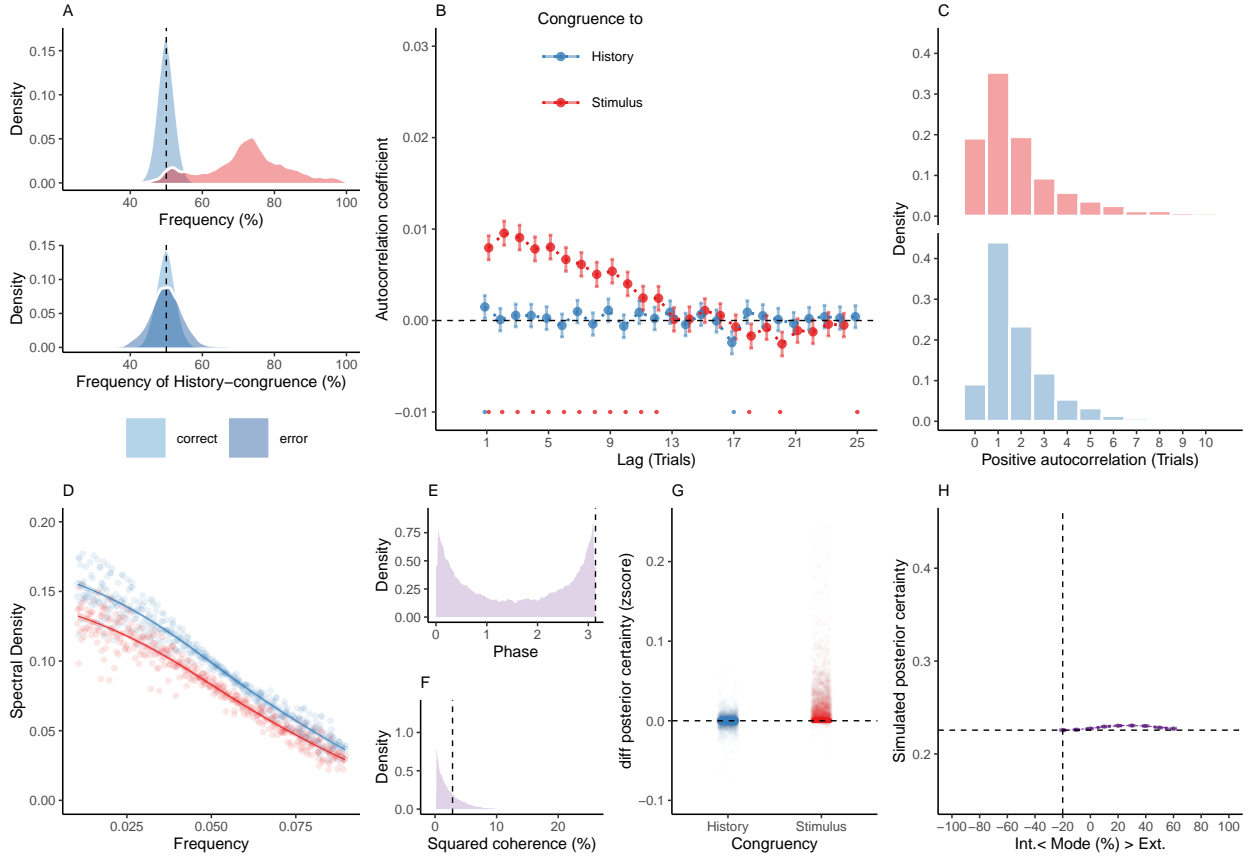
E. In the normative-evidence-accumulation model, the distribution of phase shift between fluctuations in simulated stimulus- and history-congruence peaked at half a cycle (π denoted by dotted line). In contrast to the full model, the dynamic probabilities of simulated stimulus- and history-congruence were positively correlated ($\beta = 4.3 \times 10^{-3} \pm 7.97 \times 10^{-4}$, $T(1.98 \times 10^6) = 5.4$, $p = 6.59 \times 10^{-8}$).

F. In the normative-evidence-accumulation model, the average squared coherence between fluctuations in simulated stimulus- and history-congruence (black dotted line) was reduced in comparison to the full model ($T(3.52 \times 10^3) = -6.27$, $p = 3.97 \times 10^{-10}$) and amounted to $3.26 \pm 8.88 \times 10^{-4}\%$.

G. Similar to the full bimodal inference model, confidence simulated from the no-oscillation model was enhanced for stimulus-congruent choices ($\beta = 0.01 \pm 1.05 \times 10^{-4}$, $T(2.1 \times 10^6) = 139.17$, $p < 2.2 \times 10^{-308}$) and history-congruent choices ($\beta = 8.05 \times 10^{-3} \pm 9.2 \times 10^{-5}$, $T(2.1 \times 10^6) = 87.54$, $p < 2.2 \times 10^{-308}$).

H. In the normative-evidence-accumulation model, the positive quadratic relationship between the mode of perceptual processing and confidence was markedly reduced in comparison to the full model ($\beta_2 = 0.14 \pm 0.07$, $T(2.1 \times 10^6) = 1.95$, $p = 0.05$). The horizontal and vertical dotted lines indicate minimum posterior certainty and the associated mode, respectively.

0.13 Supplemental Figure S13



Supplemental Figure S13. Reduced Control Model M5: No accumulation of information across trials. When simulating data for the *no-evidence-accumulation model*, we removed the accumulation of information across trials by setting the Hazard rate H to 0.5. Simulated data thus depended only on the participant-wise estimates for the amplitudes $a_{LLR/\psi}$, frequency f , phase p and inverse decision temperature ζ .

A. Similar to the full model (Figure 1F and Figure 4), simulated perceptual choices were stimulus-congruent in $72.14\% \pm 0.17\%$ of trials (in red). History-congruent amounted to $49.89\% \pm 0.03\%$ of trials (in blue). In contrast to the full model, the no-accumulation model showed a significant bias against perceptual history $T(4.32 \times 10^3) = -3.28$, $p = 1.06 \times 10^{-3}$; upper panel). In contrast to the full model, there was no difference in the frequency of history-congruent choices between correct and error trials ($T(4.31 \times 10^3) = 0.76$, $p = 0.44$; lower panel).

B. In the no-evidence-accumulation model, we found no significant autocorrelation of history-congruence beyond the first trial, whereas the autocorrelation of stimulus-congruence was preserved.

C. In the no-evidence-accumulation model, the number of consecutive trials at which true autocorrelation coefficients exceeded the autocorrelation coefficients for randomly permuted data increased with respect to stimulus-congruence ($2.83 \pm 1.49 \times 10^{-3}$ trials; $T(4.31 \times 10^3) = 3.45$, $p = 5.73 \times 10^{-4}$) and decreased with respect to history-congruence ($1.85 \pm 3.49 \times 10^{-4}$ trials; $T(4.32 \times 10^3) = -19.37$, $p = 3.49 \times 10^{-80}$) relative to the full model.

D. In the no-evidence-accumulation model, the smoothed probabilities of stimulus- and history-congruence (sliding windows of ± 5 trials) fluctuated as a scale-invariant process with a $1/f$ power law, i.e., at power densities that were inversely proportional to the frequency (power $\sim 1/f^\beta$; stimulus-congruence: $\beta = -0.82 \pm 1.2 \times 10^{-3}$, $T(1.92 \times 10^5) = -681.98$, $p < 2.2 \times 10^{-308}$; history-congruence: $\beta = -0.78 \pm 1.11 \times 10^{-3}$, $T(1.92 \times 10^5) = -706.57$, $p < 2.2 \times 10^{-308}$).

E. In the no-evidence-accumulation model, the distribution of phase shift between fluctuations in simulated stimulus- and history-congruence peaked at half a cycle (π denoted by dotted line). In contrast to the full model, the dynamic probabilities of simulated stimulus- and history-congruence were not significantly anti-correlated ($\beta = 6.39 \times 10^{-4} \pm 7.22 \times 10^{-4}$, $T(8.89 \times 10^5) = 0.89$, $p = 0.38$).

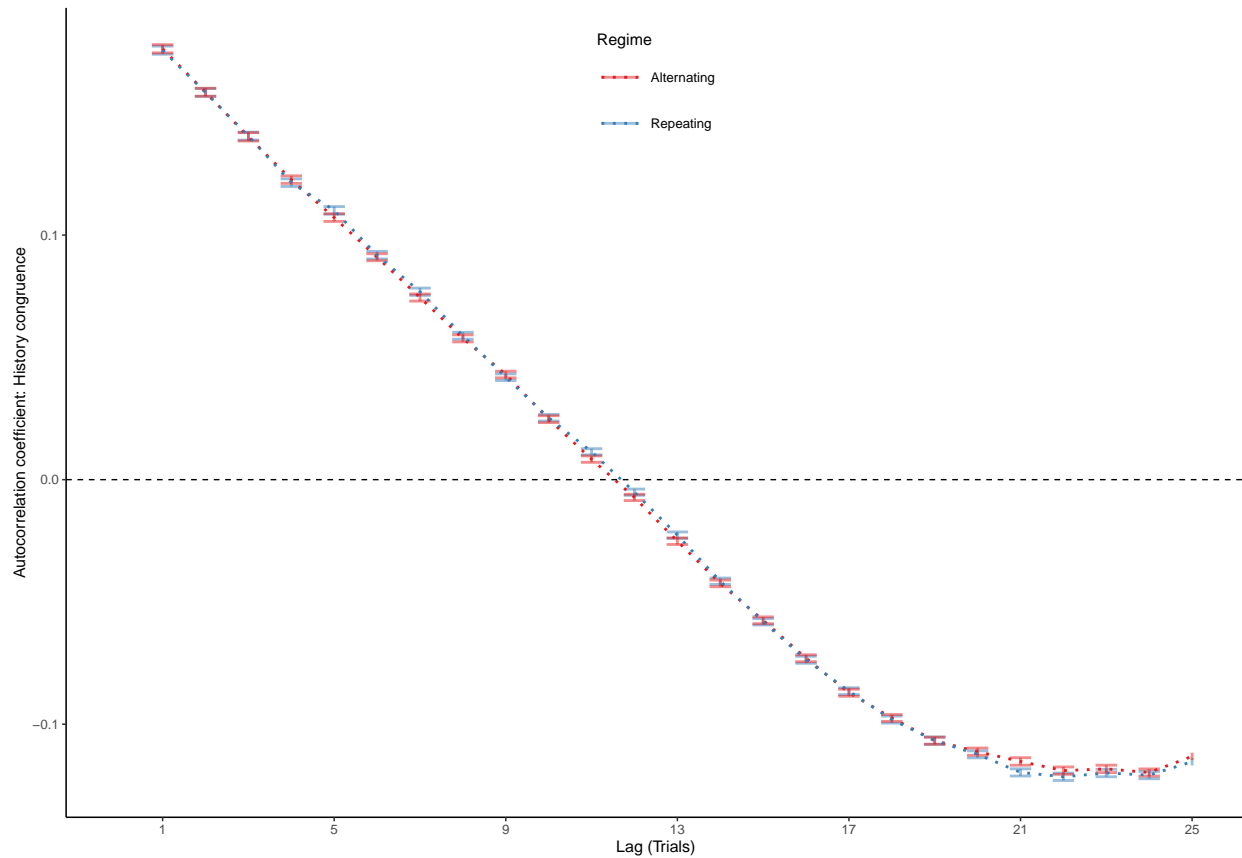
F. In the no-evidence-accumulation model, the average squared coherence between fluctuations in simulated stimulus- and history-congruence (black dotted line) was reduced in comparison to the full model ($T(3.56 \times 10^3) = -9.96$, $p = 4.63 \times 10^{-23}$) and amounted to $2.8 \pm 7.29 \times 10^{-4}\%$.

G. Similar to the full bimodal inference model, confidence simulated from the no-evidence-accumulation model was enhanced for stimulus-congruent choices ($\beta = 0.01 \pm 9.4 \times 10^{-5}$, $T(2.11 \times 10^6) = 158.1$, $p < 2.2 \times 10^{-308}$). In contrast to the full bimodal inference model, history-congruent choices were not characterized by enhanced confidence ($\beta = 8.78 \times 10^{-5} \pm$

$$8.21 \times 10^{-5}, T(2.11 \times 10^6) = 1.07, p = 0.29).$$

H. In the no-evidence-accumulation model, the positive quadratic relationship between the mode of perceptual processing and confidence was markedly reduced in comparison to the full model ($\beta_2 = 0.19 \pm 0.06$, $T(2.11 \times 10^6) = 3$, $p = 2.69 \times 10^{-3}$). The horizontal and vertical dotted lines indicate minimum posterior certainty and the associated mode, respectively.

0.14 Supplemental Figure S14



Supplemental Figure S14. Autocorrelation of history-congruence of alternating and repeating biases. Here, we simulate the autocorrelation of history-congruence in 10^3 synthetic participants. In the repeating regime (blue), history-congruence fluctuated between 50% and 80% (blue) in interleaved blocks (10 blocks per condition with a random duration between 15 and 30 trials). In the alternation regime (red), history-congruence fluctuated between 50% and 20%. The resulting autocorrelation curves for history-congruence overlap, indicating that our analysis is able to accommodate both repeating and alternating biases.

0.15 Supplemental Table T1

Authors	Journal	Year
Bang, Shekhar, Rahnev	JEP:General	2019
Bang, Shekhar, Rahnev	JEP:General	2019
Calder-Travis, Charles, Bogacz, Yeung	Unpublished	NA
Clark & Merfeld	Journal of Neurophysiology	2018
Clark	Unpublished	NA
Faivre, Filevich, Solovey, Kuhn, Blanke	Journal of Neuroscience	2018
Faivre, Vuillaume, Blanke, Cleeremans	bioRxiv	2018
Filevich & Fandakova	Unplublished	NA
Gajdos, Fleming, Saez Garcia, Weindel, Davranche	Neuroscience of Consciousness	2019
Gherman & Philiastides	eLife	2018
Haddara & Rahnev	PsyArXiv	2020
Haddara & Rahnev	PsyArXiv	2020
Hainguerlot, Vergnaud, & de Gardelle	Scientific Reports	2018
Hainguerlot, Gajdos, Vergnaud, & de Gardelle	Unpublished	NA
Jachs, Blanco, Grantham-Hill, Soto	JEP:HPP	2015
Jachs, Blanco, Grantham-Hill, Soto	JEP:HPP	2015
Jachs, Blanco, Grantham-Hill, Soto	JEP:HPP	2015
Jaquiere, Yeung	Unpublished	NA
Kvam, Pleskac, Yu, Busemeyer	PNAS	2015
Kvam, Pleskac, Yu, Busemeyer	PNAS	2015
Kvam and Pleskac	Cognition	2016
Law, Lee	Unpublished	NA
Lebreton, et al.	Sci. Advances	2018
Lempert, Chen, & Fleming	PlosOne	2015
Locke*, Gaffin-Cahn*, Hosseiniaveh, Mamassian, & Landy	Attention, Perception, & Psychophysics	2020
Maniscalco, McCurdy,Odegaard, & Lau	J Neurosci	2017
Maniscalco, McCurdy,Odegaard, & Lau	J Neurosci	2017
Maniscalco, McCurdy,Odegaard, & Lau	J Neurosci	2017
Maniscalco, McCurdy,Odegaard, & Lau	J Neurosci	2017
Martin, Hsu	Unpublished	NA
Massoni & Roux	Journal of Mathematical Psychology	2017
Massoni	Unpublished	NA
Mazor, Friston & Fleming	eLife	2020
Mei, Rankine,Olafsson, Soto	bioRxiv	2019
Mei, Rankine,Olafsson, Soto	bioRxiv	2019
O'Hora, Zgonnikov, Kenny, Wong-Lin	Fechner Day proceedings	2017
O'Hora, Zgonnikov, CiChocki	Unpublished	NA

(continued)

Authors	Journal	Year
O'Hora, Zgonnikov, Neverauskaite	Unpublished	NA
Palser et al	Consciousness & Cognition	2018
Pereira, Faivre, Iturrate et al.	bioRxiv	2018
Prieto et al.	Submitted	NA
Rahnev et al	J Neurophysiol	2013
Rausch & Zehetleitner	Front Psychol	2016
Rausch et al	Attention, Perception, & Psychophysics	2018
Rausch et al	Attention, Perception, & Psychophysics	2018
Rausch, Zehetleitner, Steinhauser, & Maier	NeuroImage	2020
Recht, de Gardelle & Mamassian	Unpublished	NA
Reyes et al.	PlosOne	2015
Reyes et al.	Submitted	NA
Rouault, Seow, Gillan, Fleming	Biol. Psychiatry	2018
Rouault, Seow, Gillan, Fleming	Biol. Psychiatry	2018
Rouault, Dayan, Fleming	Nat Commun	2019
Sadeghi et al	Scientific Reports	2017
Schmidt et al.	Consc Cog	2019
Shekhar & Rahnev	J Neuroscience	2018
Shekhar & Rahnev	PsyArXiv	2020
Sherman et al	Journal of Neuroscience	2016
Sherman et al	Journal of Cognitive Neuroscience	2016
Sherman et al	Unpublished	NA
Sherman et al	Unpublished	NA
Siedlecka, Wereszczyski, Paulewicz, Wierzchon	bioRxiv	2019
Song et al	Consciousness & Cognition	2011
van Boxtel, Orchard, Tsuchiya	bioRxiv	2019
van Boxtel, Orchard, Tsuchiya	bioRxiv	2019
Wierzchon, Paulewicz, Asanowicz, Timmermans & Cleeremans	Consciousness and Cognition	2014
Wierzchon, Anzulewicz, Hobot, Paulewicz & Sackur	Consciousness and Cognition	2019

0.16 Supplemental Table T2

Parameters	Interpretation
α	Sensitivity to sensory information
H	Expected probability of a switch in the cause of sensory information (Hazard)
a_{LLR}	Amplitude of fluctuations in likelihood precision ω_{LLR}
a_ψ	Amplitude of fluctuations in prior precision ω_ψ
f	Frequency of ω_{LLR} and ω_ψ
p	Phase (p for ω_{LLR} ; p + π for ω_ψ)
ζ	Inverse decision temperature